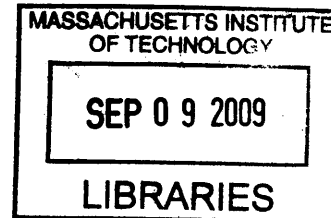


Potential Technologies Based on Stamped Periodic Nanoparticle Array

by

Zongbin Wang

B.Eng. (Hons), Materials Engineering (2007)
Nanyang Technological University



Submitted to the Department of Materials Science and Engineering
in Partial Fulfillment of the Requirements for Degree of
Master of Engineering in Materials Science and Engineering
at the

Massachusetts Institute of Technology

September 2009

© 2009 Massachusetts Institute of Technology.

All rights reserved

ARCHIVES

Signature of Author
Department of Materials Science and Engineering
July 29, 2009

Certified by
Carl V. Thompson
Professor of Department of Materials Science and Engineering
Thesis Supervisor

Handwritten signature of Carl V. Thompson in black ink.

Accepted
Christine Ortiz
Chair, Departmental Committee on Graduate Students

Handwritten signature of Christine Ortiz in black ink.

Potential Technologies Based on Stamped Periodic Nanoparticle Array

by
Zongbin Wang

Submitted to the Department of Materials Science and Engineering
on July 29, 2009 in Partial Fulfillment of the Requirements for Degree of
Master of Engineering in Materials Science and Engineering

ABSTRACT

A stamped nanoparticle array patterning technology integrating interference lithography, self assembly and soft lithography is assessed. This technology is capable of parallel patterning of nanoparticles at a large scale. Among several possible applications of this technology, potential for Deoxyribonucleic Acid detection is specifically investigated. Attaching DNA to nanoparticles through a probe molecule changes the local dielectric environment and hence affects surface plasmon resonance. However, the projected plasmon peak shift is not significant. Another detection method is described here to create a visible optical DNA sensor with a tolerable increase in cost relative to existing technologies. Intellectual property issues are also discussed for this technology.

Thesis Supervisor: Carl V. Thompson

Title: Stavros Salapatas Professor of Materials Science and Engineering

Acknowledgement

There are a lot of people who have been helping me, both in academic and personal growth. I am grateful to everyone. Firstly, I would like to thank Professor Thompson and Professor Choi for their guidance. They have always been encouraging and helpful along the way. Their valuable advice made preparation of this thesis much easier. My classmates are always cheerful. Discussion with them inspired my learning along the whole M.Eng course. Finally, I would like to thank my parents. It is their unconditional love and support that have been driving me so far.

Table of Contents

ABSTRACT	2
Acknowledgement	3
List of Figures	6
List of Tables	7
1. Introduction	8
2. Technology	10
2.1. Interference Lithography	10
2.2. Metallic Thin Film Dewetting Self Assembly	12
2.2.1. Rayleigh Instability	12
2.2.2. Metallic Thin Film Dewetting	13
2.2.3. Gold Nanoparticle Array by Templated Dewetting	14
2.3. Soft Lithography	16
2.3.1. Elastomeric Stamp	16
2.3.2. SAM Microcontact Printing Process	18
2.3.3. Nano Transfer Printing	21
2.4. The Proposed Technology	24
2.4.1. Method 1	24
2.4.2. Method 2	24
2.4.3. Method 3	25
3. Potential Applications	26
4. Current Nanoparticle Based DNA Detection	28
4.1. Quartz Crystal Microbalance (QCM)	28
4.2. Electrical Detection	29
4.3. Optical Detection	29
5. Optical DNA Sensor Application of Stamped Nanoparticle Array	31
5.1. Modeling by Electromagnetism for Single Gold Nanoparticle	31
5.2. Previous Experimental Work on Single Nanoparticle	34
5.3. Modeling by Fourier Modal Method (FMM) for Nanoparticle Arrays	37
5.4. Au Nanoparticle Array and Colloidal Combined DNA Sensor	39

6. Intellectual Property Assessment.....	42
7. Conclusion.....	44
8. References	45
9. Appendix	48
Cost Model	48

List of Figures

Figure 2-1 Interference lithography system [3].....	10
Figure 2-2 Interference of two plane wave[6].....	10
Figure 2-3 Fringes patterned by Interference Lithography[7].....	11
Figure 2-4 Inverted pyramids in Si produced by interference lithography.[3].....	12
Figure 2-5 Rayleigh instability decompose liquid cylinder into droplets[10].....	13
Figure 2-6 Void formation at grain boundary [12].....	13
Figure 2-7 Void growth in dewetting process [12].....	14
Figure 2-8 Au nanoparticles in inverted pyramid array in Si substrate by templated dewetting [13]	14
Figure 2-9 Fabrication process of Au nanoparticle arrays in inverted pyramids [14].....	15
Figure 2-10 SEM of Au nanoparticles in Si inverted pyramids [14].....	15
Figure 2-11 PDMS structure.....	16
Figure 2-12 Stamp with rectangular cross section roof recess, and common failure modes during μ CP. [24]	17
Figure 2-13 Fabrication of two-layer composite PDMS stamp (Top layer, soft PDMS; Bottom thin layer, hard PDMS)[27]	18
Figure 2-14 Defect and width of pattern vs. concentration of ink solution[28]	19
Figure 2-15 Schematic depicting μ CP process [16].....	21
Figure 2-16 Optical micrograph of gold patterned by nTP on (a) silicon wafer, (b) PET [33].....	21
Figure 2-17 Schematic illustration of nanotransfer printing (nTP) on GaAs: (a) Native oxide is removed from wafer surface before 1,8-octanedithiol SAM is deposited; (b) a gold coated PDMS stamp is brought into contact with treated surface; (c) stamp is removed [35].....	22
Figure 2-18 (a) InP micro structure inked on stamp and transfer-printed on plastic substrate; (b) Optical Micro Trilayer of GaAs nanowires on a plastic substrate. [39].....	23
Figure 2-19 Proposed technology: Method 1	24
Figure 2-20 Proposed technology: Method 2	24
Figure 2-21 Proposed Technology: Method 3	25
Figure 4-1 Procedure of amplified assay of a target DNA by oligonucleotide-capped gold nanoparticle using Quartz Crystal Microbalance detection [47].....	29

Figure 4-2 DNA assay by electrical detection [48]29

Figure 4-3 Schematic of optical detection of DNA: substrate is glass; silver ion is added to enhance the contrast [49].....30

Figure 5-1 Plasmon oscillation for a sphere [53]32

Figure 5-2 Dark field illumination with 100X objective lens (A) before immersion in oil and (B) during immersion in oil (n=1.44) [55].....35

Figure 5-3 Spectra of an individual particle 1(blue, roughly spherical) (a) before, (b) during, and (c) after exposure to thin film of 1.44 index oil [55].....36

Figure 5-4 Illustration of single Au nanoparticle as streptavidin sensor [54]36

Figure 5-5 Comparison of scattering spectrum before (solid line) and after (dashed line) adding streptavidin [54].....37

Figure 5-6 (a) Schematic description of bi-periodic gold nanoparticle array on a glass substrate, the particles are cylindrical with 100nm diameter and 20nm height; (b) Cross section of one period, covered with a layer of dielectric coating with refractive index of 1.4 [62]38

Figure 5-7 Effect of local dielectric environment calculated on optical extinction [62].....39

Figure 5-8 Schematic of proposed DNA sensor with combined nanoparticle array and colloid (Drawing is not to scale).....40

Figure 5-9 Modeled unit cost versus production volume41

Figure 9-1 Modeled unit cost versus production volume48

List of Tables

Table 1 Summary of SAM μ contact printing process [22] 19

Table 2 Information used in cost modeling49

1. Introduction

A lot of research interest and effort have been directed to nanoscience and nanotechnology in the past two decades. Nanostructure fabrication technology has advanced significantly with size control, position control, variety of materials etc.. Many embodiments of top down and bottom up approaches have been developed. More engineering controlled systems tend to require synergy of top down and bottom up technologies.

Optical lithography has been advancing for a long way driven by mainly semiconductor industry, with resolution improved to sub 100 nm in production. However, the cost remains high; typical lithography machine costs tens of millions of dollars. Further miniaturization is believed to be achievable with extreme ultraviolet (wavelength 121 nm–10 nm), listed in International Technology Roadmap for Semiconductors [1]. Absorbance increases as wavelength moves to extreme ultraviolet; equipment cost is expected to grow further because of more complexity in optic system. In addition, reticle cost will increase as well. Interference lithography patterns array of materials by interference of coherent light beams [2, 3]. It is a mask free, low cost lithography technique capable of large scale parallel patterning.

Self assembly refers to a spontaneous process in which components/atoms assemble themselves driven by interaction among themselves and environment. Engineering controlled self assembly process can be utilized to fabricate lithography-free nanostructures as a bottom up approach. The interaction during self assembly is usually weak and in short range. Hence, such nano structures do not have long range order. A template offers an external driving force or guide to impart long range order in the self assembled structures [4].

Soft lithography refers to a family of techniques to fabricate or replicate structures using an elastomeric stamp, mold or conformal photomask [5]. It is capable of patterning materials/structures at micrometer to nanometer scale. It has advantages like low cost, better conformability to non-planar surfaces, simplicity in process, biocompatibility etc.. Various soft lithography techniques have been developed.

Integrating interference lithography, self assembly and soft lithography, a stamped nanoparticle array fabrication method is proposed by Professor Carl Thompson, Professor Wee Kiong Choi and Professor Xiaogang Liu from Singapore-MIT Alliance. It combines top down and bottom up approaches and patterns nanoparticle array with periodicity down to 200 nm. It enables parallel nanoparticle fabrication on large scale substrate.

It is important to assess a new technology in advance so that the research is more targeted. The objective of this project is to evaluate the viability and potential of this technology on engineering applications. There are several potential applications for this stamped nanoparticle array technology. This paper focuses on its potential in biosensor application, DNA sensor in specific.

2. Technology

The proposed technology reviewed in this project synergizes interference lithography, self assembly and soft lithography to fabricate nanoparticle array. This chapter firstly presents these technologies, and then discusses how these technologies can be integrated to fabricate stamped periodic nanoparticle array.

2.1. Interference Lithography

Interference lithography uses interference of two or more coherent light beams to produce periodic patterns[2, 3]. Figure 2-1 depicts typical interference lithography equipment [3].

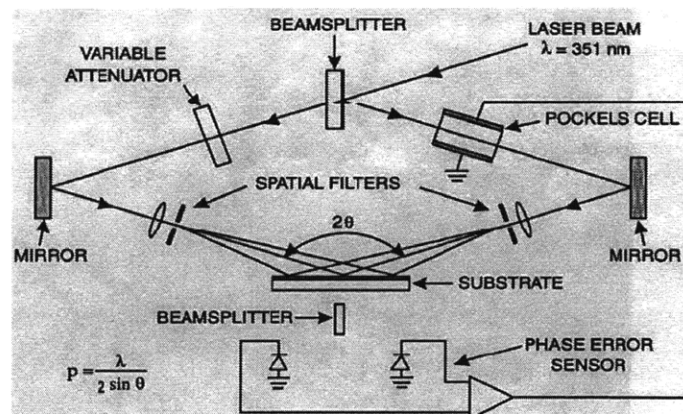


Figure 2-1 Interference lithography system [3]

Because of interference, a standing wave forms as two coherent light beams meet (Figure 2-2).

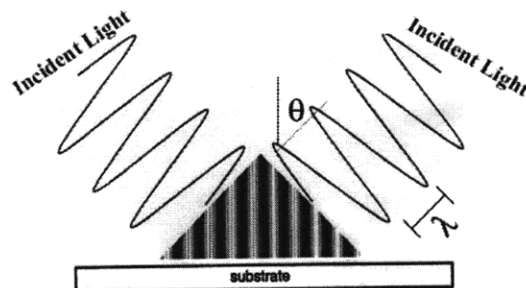


Figure 2-2 Interference of two plane wave[6]

Fringes of light intensity maxima and minima can be recorded by photoresist as shown in Figure 2-3.

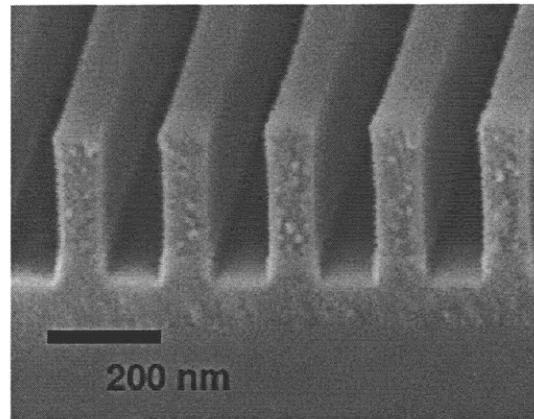


Figure 2-3 Fringes patterned by Interference Lithography[7]

The period of structure is determined by equation:

$$p = \frac{\lambda}{2 \cdot \sin\theta}$$

Depending on wavelength of laser source and equipment setup, the period of patterns can be as small as around 200 nm, smaller than visible light spectrum.

Dual exposures on the photoresist with 90 degree planar rotation produce an ordered array of square patterns in the photoresist. The KOH wet etching rate along silicon [111] direction is slower than that along [100] direction. Because of anisotropy in etching rate, subsequent wet etching with KOH transfers the square array pattern into an array of inverted pyramids on a (100) silicon substrate, as shown in Figure 2-4.

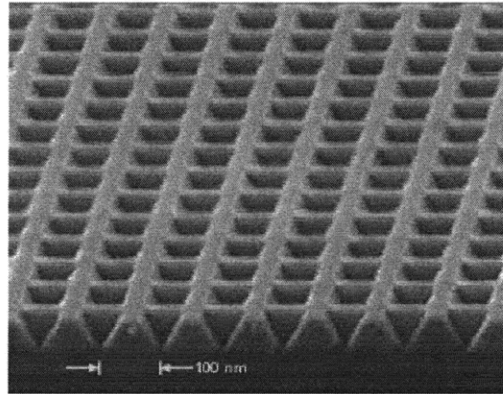


Figure 2-4 Inverted pyramids in Si produced by interference lithography.[3]

Interference lithography patterns arrays of fine features in large scale, without use of complex optic system. It is also a mask-free technique. It has advantage in cost compared to other lithography techniques like electron beam or dip pen lithography.

2.2. Metallic Thin Film Dewetting Self Assembly

2.2.1. Rayleigh Instability

Metallic thin film dewetting process is analogous to Rayleigh instability [8]. Rayleigh modeled an infinite wire made of liquid and found that it is unstable against perturbations with wavelength larger than a critical value $\lambda=2\pi R$, where R is radius of the cylinder. A liquid wire will decompose to small liquid droplets (Figure 2-5). The driving force is minimization of surface energy. Theoretical analysis shows that there is a kinetically favored characteristic wavelength, $\lambda_m = 9.016R$.

Further study by Nichols and Mullins shows that isolated solid wire experiences identical instability growth [9]. Solid wire is also unstable against perturbations with wavelength λ larger than $2\pi R$; there is a characteristic wavelength dominating the process kinetically as well. The difference is that the instability grows mainly by surface diffusion, not hydrodynamic flow.

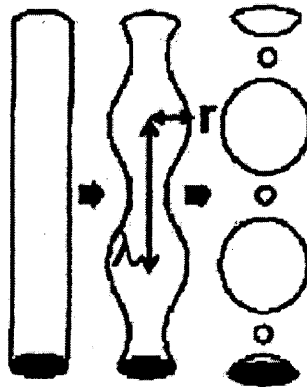


Figure 2-5 Rayleigh instability decompose liquid cylinder into droplets[10]

2.2.2. Metallic Thin Film Dewetting

A perfect film is stable against perturbations with any wavelength, as studied by Mullins [11]. Film will not decompose unless the perturbation is deep enough to penetrate through. Polycrystalline film like metal film has defects like grain boundaries.

Jiran and Thompson analyzed the dewetting process of Au thin film deposited by electron beam evaporation [12]. According to the dewetting model proposed, dewetting process happens in two steps: void formation (Figure 2-6) and growth (Figure 2-7). Fluctuations occur at grain boundaries; grooves can develop at grain boundary triple junctions (Figure 2-6a, b). If the groove is large enough to reach the substrate and contact angle is large enough, a stable void forms in the film (Figure 2-6c). The growth of the void is then driven by the reduction of the curvature at the film edge. The film becomes discontinuous when voids impinge and islands of material form. These islands will evolve into equilibrium shapes such as spherical caps (Figure 2-7).

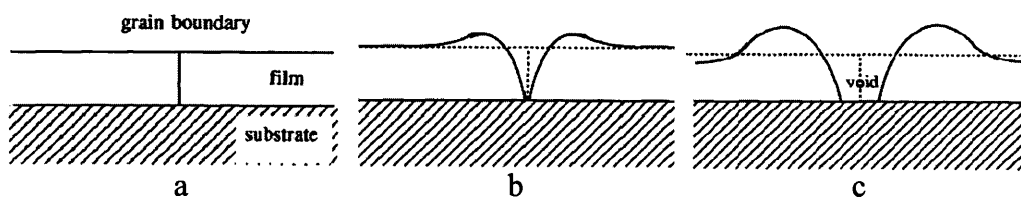


Figure 2-6 Void formation at grain boundary [12]

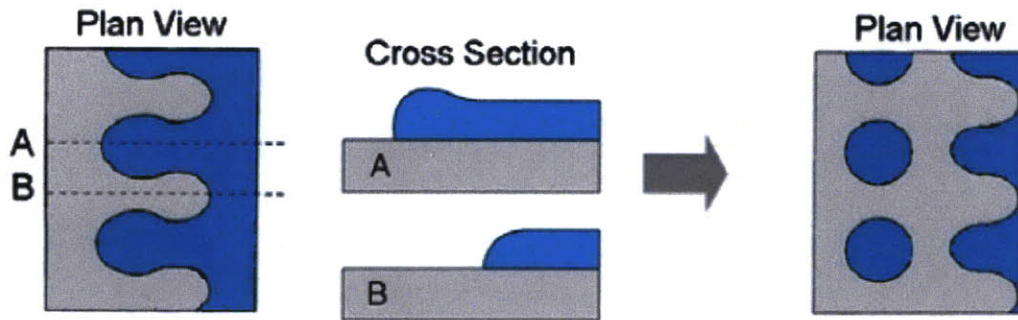


Figure 2-7 Void growth in dewetting process [12]

2.2.3. Gold Nanoparticle Array by Templated Dewetting

Dewetting can be controlled as a self assembly process to fabricate nano particles. However, the particle position and size are not controlled. A template, either topographical or chemical, adds position and size control to the self assembly process. Giemann and Thompson used array of inverted pyramids in Si patterned by interference lithography (Figure 2-4b) to template dewetting of Au film. Ordered nano particle arrays form, as depicted in Figure 2-8 [13].

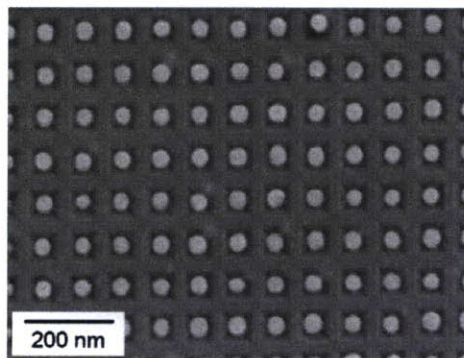


Figure 2-8 Au nanoparticles in inverted pyramid array in Si substrate by templated dewetting [13]

Choi and Thompson et al. then developed the Au nanoparticle array fabrication method based on dewetting of Au film on inverted pyramid array template, with addition of silicon oxide overhang structure [14]. Figure 2-9 illustrates the fabrication process. A silicon oxide layer is

introduced to make an overhang structure above the inverted pyramid (Figure 2-9b), so that the Au film deposited is not continuous.

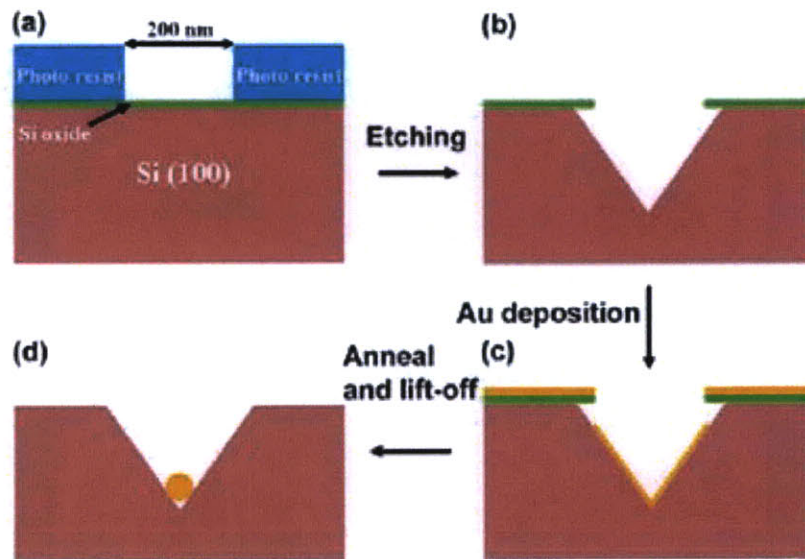


Figure 2-9 Fabrication process of Au nanoparticle arrays in inverted pyramids [14]

The silicon oxide layer also acts as a lift off mask to get rid of excessive Au outside the inverted pyramids. Gold film is no longer continuous and only exists inside the inverted pyramids. Subsequent dewetting leads to fine Au nanoparticles in the inverted pyramids, as shown in Figure 2-10.

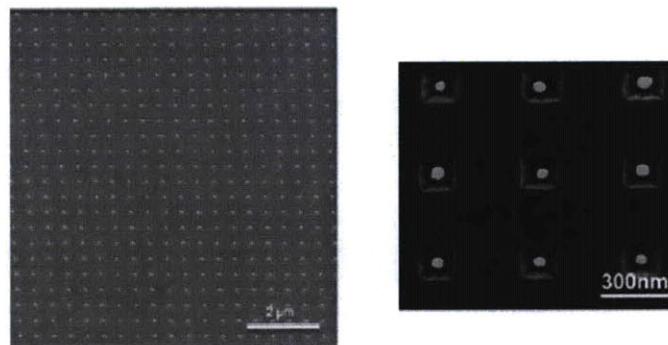


Figure 2-10 SEM of Au nanoparticles in Si inverted pyramids [14]

2.3. Soft Lithography

Soft lithography is a family of techniques for fabricating or replicating structures using elastomeric stamps, molds, and conformable masks. Development of soft lithography expanded rapidly during last decades, with its capability patterning structures at lateral dimensions down to 20 nm[15, 16]. It provides advantages like low cost, high throughput, mask-free. Soft Lithography techniques includes microcontact printing (μ CP)[17], nano transfer printing (nTP)[5], replica molding (REM)[18], microtransfer molding (mTM)[19], micromolding in capillaries (MIMIC)[20], and solvent-assisted micromolding (SAMIM)[21] etc.. Among them, nano transfer printing (nTP) can be used to transfer nano-sized features directly in an additive way. Self Assembled Monolayers (SAMs) patterning by microcontact printing is also of great interest in the proposed nanoparticle array stamping patterning technology, as the SAM patterns generated can be used as template for further process at nano scale, such as etch mask, selective crystallization sites, chemical template etc..

2.3.1. Elastomeric Stamp

The stamp used for soft lithography is usually poly(dimethylsiloxane) (PDMS). PDMS is a commercially available silicone rubber.

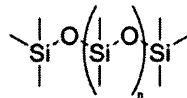


Figure 2-11 PDMS structure

Elasticity of stamp makes microcontact printing conformal, hence molecular contacting to substrate surface. Composition of precursor and curing agent, reaction temperature and time, directly affect degree of crosslinking, hence Young's modulus of PDMS. Too much elasticity will lead to poor spatial features printed. Early work on microcontact printing uses PDMS with

low Young's modulus around 1 to 3 MPa; the material is too soft and cannot define features smaller than 500 nm due to deformation.[22] The common deformations are buckling, lateral collapse and roof collapse[23], as shown in Figure 2-12[24].

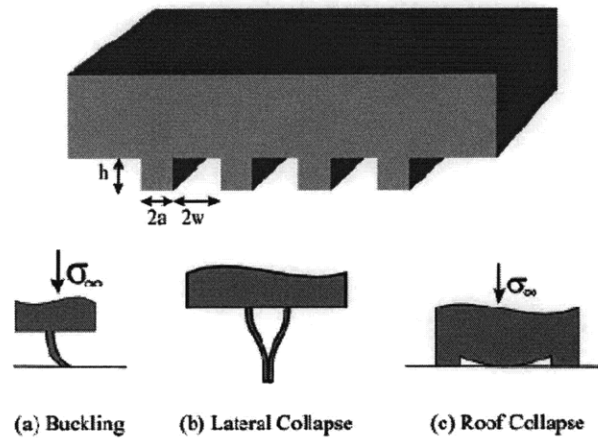


Figure 2-12 Stamp with rectangular cross section roof recess, and common failure modes during μ CP. [24]

Theoretical models based on continuum mechanics can be used to accurately predict physical deformation of the stamp during microcontact printing process[25]. Sharp et al. used theoretical modeling and experiment to study the three failure modes[24]. Critical condition to avoid printing failures:

$$\frac{-4\sigma_{\infty}w}{\pi E^* h} \left(1 + \frac{a}{w}\right) \cosh^{-1} \left[\sec \left(\frac{w\pi}{2(w+a)} \right) \right] < 1$$

(roof collapse)

$$\frac{-12\sigma_{\infty}h^2}{\pi^2 E^* a^2} < \frac{1}{1 + (w/a)}$$

(buckling)

$$\frac{h}{2a} \left[\frac{4\gamma_s}{3E^* a} \right]^{1/4} < \sqrt{w/a}$$

(lateral collapse)

where E^* is plane strain modulus: $E^* \equiv \frac{E}{1-\nu^2}$, E is Young's modulus, ν is Poisson's ratio. σ_∞ is the uniform stress applied to top of stamp, γ_s is the surface energy of stamp material, w , a , h are dimension of stamp feature in Figure 2-12.

Although the above analysis is for PDMS stamp features with rectangular cross sections, the message behind is that to avoid mechanical failure, it is favorable to use stamp materials with a higher Young's modulus. This is also true for PDMS stamp casted with pyramid structure.

Further research efforts increases PDMS the Young's modulus around 9.7 MPa, which made 20 nm replicate structure possible[26]; but it is too fragile to be used as a stamp and has poor conformability to substrate surface curvature. A two-layer composite stamp structure, as shown in Figure 2-13, keeps flexibility as well as well defined surface features down to 50 nm [27].

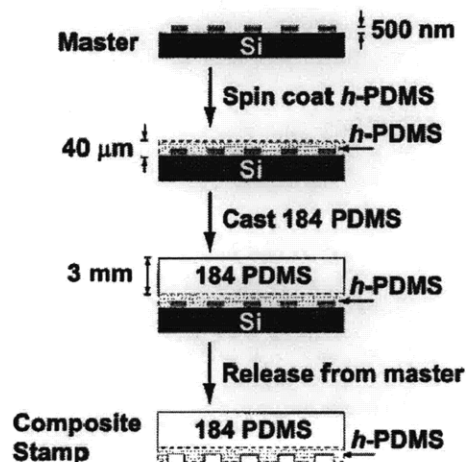


Figure 2-13 Fabrication of two-layer composite PDMS stamp (Top layer, soft PDMS; Bottom thin layer, hard PDMS)[27]

2.3.2. SAM Microcontact Printing Process

Table 1 presents a typical Self Assembled Monolayer (SAM) microcontact printing process with molecule “inked” by immersion [22]. Although there are different ‘inking’ processes developed for SAM μ CP, immersion is still the most common technique.

Table 1 Summary of SAM μ contact printing process [22]

Process	Inking		Stamping		
	Immersion	Drying	Initial contact and propagation	Self assembly full contact	Peeling off
Time	30 ~ 60 sec	10 ~ 60 sec	1 ~ 5 sec	0.3 ~ 60 sec	1~5 sec
Failure	Swelling	Distortion	Air trapping	- Diffusion of ink	

2.3.2.1. Inking Process

There are two important parameters during immersion “inking”: immersion time and concentration of “ink”.

Concentration of ink solution affects not only the defect density but also the feature size (Figure 2-14). A high concentration can give sufficient surface coverage and lower down the defect density. But excessive lateral diffusion and vapor phase transport will lead to feature distortion. A low concentration of ink solution, hence low concentration in stamp, gives lower lateral distortion due to surface diffusion and vapor transport. However, if the surface coverage of adsorbate SAM molecule is not enough, the defect density is high.

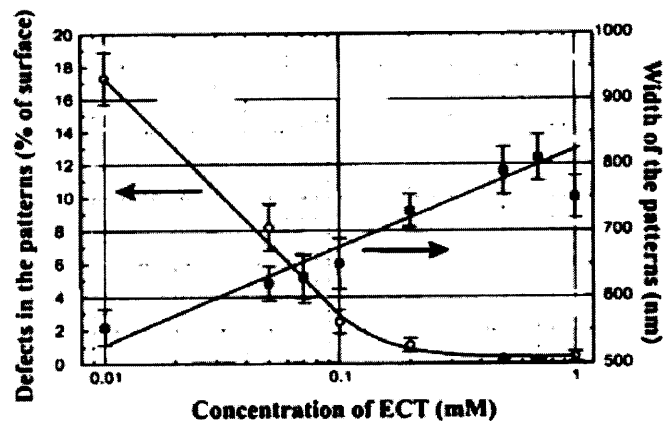


Figure 2-14 Defect and width of pattern vs. concentration of ink solution[28]

Inking time has similar effect as concentration of the ink. A short inking time will cause high defect density in SAM layer because of insufficient surface coverage. A long inking time may swell the PDMS. Swelling of the stamp during “inking” often results in the pattern increasing in size. Moreover, an excess of ink results in enhanced diffusion of the imprinted molecules on the patterned surface.

Besides immersion, other inking process has been developed. The SAM molecule has low solubility in stamp material and stays at surface [29]. In this way, swelling of stamp is minimized.

2.3.2.2. Stamping Process

The SAM μ CP process is conceptually simple: patterned stamp pre-“inked” with SAM molecule is brought into contact with substrate. During the “inking”, the molecule either wet on the stamp surface, or dissolves into stamp. The molecule will bond to substrate and assemble into a 2D crystal where stamp comes into contact with substrate. However, study shows that the actual process is much complicated and depends on stamp material, type of molecule, concentration of molecule in stamp, pressure applied, temperature, contact time, type of substrate etc. [30-32]. In most cases, the contact time is around seconds, and process varies depending on choice of stamp, SAM molecule and substrate.

There are three SAM molecule mass transport mechanisms (Figure 2-15) (1) Diffusion from stamp to substrate, (2) Surface diffusion, (3) Vapor transport [16]. The first one is important in understanding formation of SAM patterns; however, little information is known. Surface diffusion and vapor transport make lateral dimension of SAM larger than desired [32]. These two processes also contribute to SMA pattern formation on rough substrate such as polycrystalline gold [16]. The surface diffusion here refers to SAM molecule diffuse on surface of SAM layer already bonded to substrate; they diffuse towards the edge of SAM layer and bond to substrate

there. Once bonded to substrate with bonding energy typically a few eV [16], they do not diffuse extensively at room temperature (26meV)

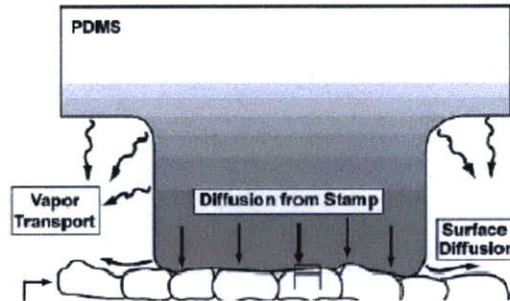


Figure 2-15 Schematic depicting μ CP process [16]

2.3.3. Nano Transfer Printing

Nano transfer printing is a soft lithography technique that transfers materials directly similar to a stamping process. In other words, it is a micro contact printing with a solid ink. Surface and interface properties are important in the transfer printing process [5]. Surface is functionalized to act as interfacial “glues” and “release” layers to control the transfer of solid inks from relief features on a stamp to a substrate [5]. With specially tailored surfaces chemistry, transfer printing of solid materials like Au has been reported [33, 34]. Figure 2-16 shows two examples of Au pattern formed by nano transfer printing on silicon and PET substrate [33].

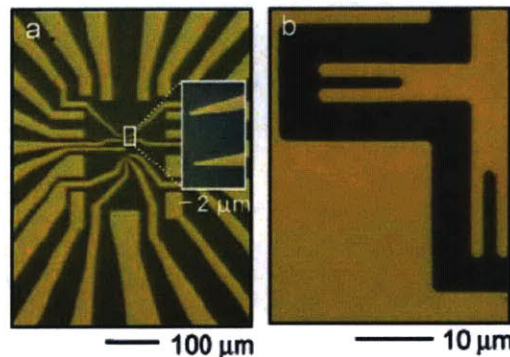


Figure 2-16 Optical micrograph of gold patterned by nTP on (a) silicon wafer, (b) PET [33]

Transfer printing requires four components: (i) a stamp with relief features in the geometry of the desired pattern; (ii) a method for depositing the ink on the stamp; (iii) a method for bringing the stamp into intimate physical contact with a substrate; and (iv) surface chemistry that prevent substantial adhesion of the deposited material to the stamp and promote its strong adhesion to the substrate [5]. In one exemplary case as depicted in Figure 2-17 [35], GaAs substrate is modified with 1,8-octanedithiol self assembled monolayer, the exposed thiol group bond gold covalently after contact. Removal of stamp causes failure at gold/PDMS interface. In this way gold ink is transfer-printed by a patterned PDMS stamp. This method is capable of generating complex patterns with nanometers resolution at large areas in a single process step.

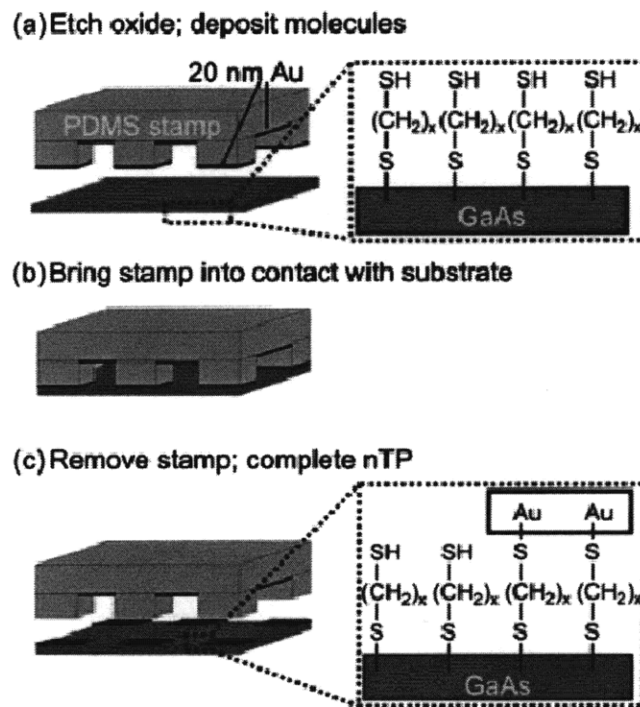


Figure 2-17 Schematic illustration of nanotransfer printing (nTP) on GaAs: (a) Native oxide is removed from wafer surface before 1,8-octanedithiol SAM is deposited; (b) a gold coated PDMS stamp is brought into contact with treated surface; (c) stamp is removed [35]

Metal, dielectric, and polymer coatings etc can be applied directly to the stamp by vapor or liquid phase deposition. Besides, a stamp can be “inked” by contacting it with a substrate that supports

the solid ink material. This approach is capable of transferring nanostructures from mother substrate where they are patterned to another substrate where they are to be used functionally. Transfer printing of nanostructures is a relatively novel form of soft lithography. There are several pioneering work reported on transfer printing of nanowires [36-39] and nanoparticle [40, 41]. In a representative case, an array of InP nanowires are pre-formed on a substrate. PDMS stamp is inked with these InP rods and then transfer printed to a plastic substrate, as shown in Figure 2-18a. Multiple-layer printing is achieved with repeated steps of transfer printing. Figure 2-18b is shows optical and scanning electron micrographs of trilayer stack of GaAs nanowires transfer printed onto a plastic substrate.

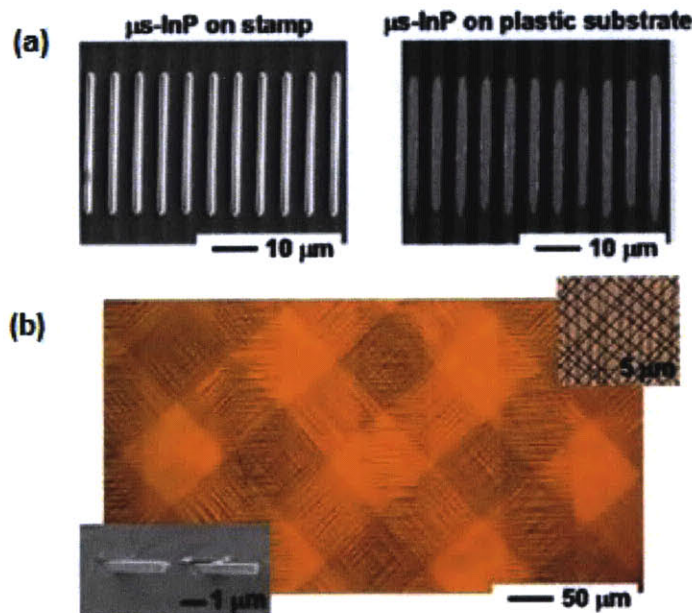


Figure 2-18 (a) InP micro structure inked on stamp and transfer-printed on plastic substrate; (b) Optical MicroTrilayer of GaAs nanowires on a plastic substrate. [39]

2.4. The Proposed Technology

There are a few proposed methods to synergize interference lithography, dewetting and other self assembly process, and soft lithography to realize stamped nanoparticle array fabrication, as explained below.

2.4.1. Method 1

- Use templated dewetting to create nanoparticle array in inverted pyramids [13, 14]
- Transfer print the nanoparticle array to a secondary substrate with PDMS stamp

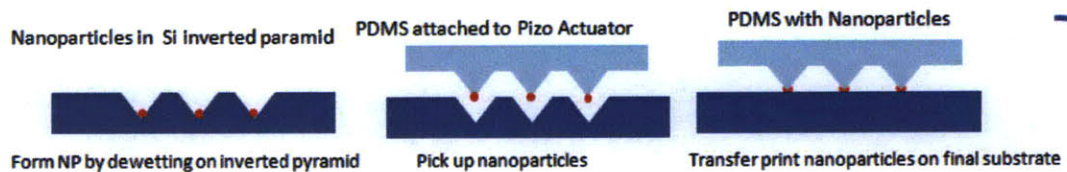


Figure 2-19 Proposed technology: Method 1

2.4.2. Method 2

- Use interference lithography to pattern inverted pyramid array in Si as a master
- Cast PDMS to make stamp
- Ink the stamp with a precursor material from a substrate and transfer print the ink to form an array
- Convert the precursor to final product by chemical reaction to form nanoparticle array.

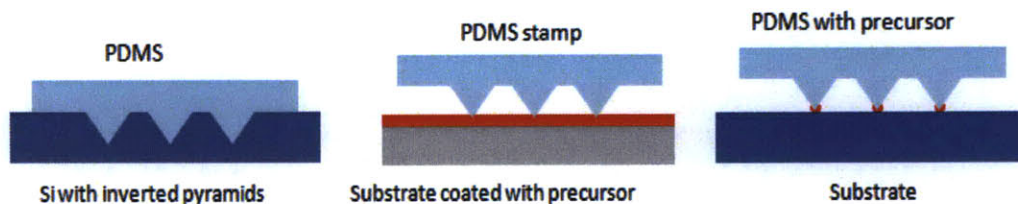


Figure 2-20 Proposed technology: Method 2

2.4.3. Method 3

- Use interference lithography to pattern inverted pyramid array in Si as a master
- Cast PDMS stamp
- Pattern self assembled monolayer array by micro contact printing
- Use the SAM array as template and form nanoparticle array either by selective nucleation from precursor[42] (Figure 2-21a) or by self assembly of existing nanoparticles from colloidal system (Figure 2-21b)

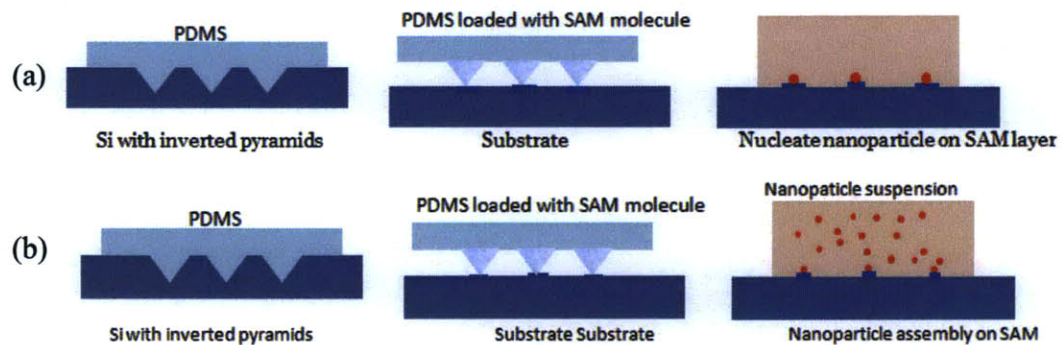


Figure 2-21 Proposed Technology: Method 3

Currently, the technology is at its very embryonic stage. Expected technology development time is around five years. There is inevitable risk and uncertainty because of the time frame and technological challenges in the development process.

3. Potential Applications

There are several potential applications for this technology, including:

- Biosensor

Metallic nanoparticle is a potential candidate for biosensor due to its optical properties determined by surface plasmon resonance. Change in surface plasmon resonance is expected if an analyte is attached to surface of nanoparticle.

- Quantum Dot to Increase LED Efficiency

Quantum confinement gives additional quantified energy levels and increases possible emission wavelength. The spatial confinement also promotes electron hole recombination and hence improves LED efficiency. If this technology can fabricate semiconducting nanoparticle epitaxial on a substrate, it can be used as cost effective quantum dot fabrication method.

- Patterned Catalyst for Nanowire/Nanotube Array Growth

Nanowires of different materials are being widely studied. Catalyst assisted Vapor-Liquid-Solid (VLS) growth method is the most common way to synthesis semiconductor nanowires. For example, silicon nanowire is grown by SiH_4 VLS method with gold as catalyst. A thin layer of Au film deposited on Si substrate is heated to high temperature. Au will dewet to form small clusters nanoparticles. SiH_4 is introduced in the reaction chamber and decomposes. There is a deep eutectic point in Au-Si phase diagram. Silicon from SiH_4 decomposition will dissolve in Au nanoparticles. As the solution supersaturates, silicon will precipitate at bottom of the particle. A continuous precipitation process leads to formation of silicon nanowire. Other nanowires and nanotubes also adopt similar growth mechanism.

The current VLS growth use metal nanoparticle/cluster from high temperature dewetting as catalyst. The position of nanowires/nanotubes is random and density is not well controlled; diameter is also dispersed. This is not as valuable as nanowires/nanotubes with controlled position in an engineering system. The stamped nanoparticle array can be used as catalyst for nanoparticle/nanotubes array growth, with precise control of position and periodicity by interference lithography.

- Nanoparticle Flash Memory

Magnetic storage media like hard disk have problems while shrinking in size. The thermal energy at service temperature must be significantly smaller than magnetocrystalline anisotropy energy and shape anisotropy energy; otherwise, magnetization of domain will fluctuate and information stored will be lost. This set a limit on minimum size of domain. In addition, the moving mechanical write/read head has reliability issues. Flash memory, on the other hand, is a type of solid state memory and does not suffer this problem. It traps charges in the floating gate. Information is stored as trapped charge at the floating gate. The trapped charge modulates the transistor and reads 0 or 1. Current flash memory used a common floating gate. It is facing reliability issues if device continues to shrink. Nanoparticle flash memory is a potential solution [43].

- Nanoparticle catalyst

Some materials show higher activity in nanoparticle form compared to their bulk [44]. Nanoparticles offer better catalytic efficiency because of increase in surface area to volume ratio and activity.

Among the possible applications, this thesis focuses on DNA detection.

4. Current Nanoparticle Based DNA Detection

There is a lot of ongoing research effort on nanoparticle based DNA sensors. Various DNA sensor architectures are being developed based on different detection mechanisms. Three typical detection mechanisms are:

4.1. Quartz Crystal Microbalance (QCM)

Quartz Crystal Microbalance (QCM) is used to monitor small addition or removal of mass on the quartz crystal resonator by monitoring the change in resonance frequency. The QCM technique is known commonly as mass measurement with sensitivity to nanogram level [45]. Change of resonance frequency and change in mass follow Sauerbrey expression [46]

$$\Delta F = -\frac{2F_0^2}{A(\mu_q Q_q)^{1/2}} \Delta m$$

where ΔF is change in resonance frequency, Δm is change in mass on the quartz crystal resonator due to material deposition or removal, μ_q and Q_q are shear modulus and density of quartz respectively, A is piezoelectrically active crystal area. The linear relationship simplifies quantified analysis.

Figure 4-1 gives an example of using nanoparticle to amplify DNA detection by quartz crystal microbalance. The quartz substrate is coated with a layer of gold, and then covered by a SAM layer, with nucleotides sequence of molecule oligo-1 conjugate to fragment of targeting DNA. Targeting DNA oligo-2 will hybridize on oligo-1. Gold nanoparticles in a colloid pre-synthesized are modified with molecule oligo-3, with nucleotides sequence of oligo-3 conjugate with fragment of targeting DNA. Nanoparticles immobilized bring significant change in mass detectable by Quartz Crystal Microbalance. In this way, the signal for DNA detection is amplified by mass of nanoparticles.

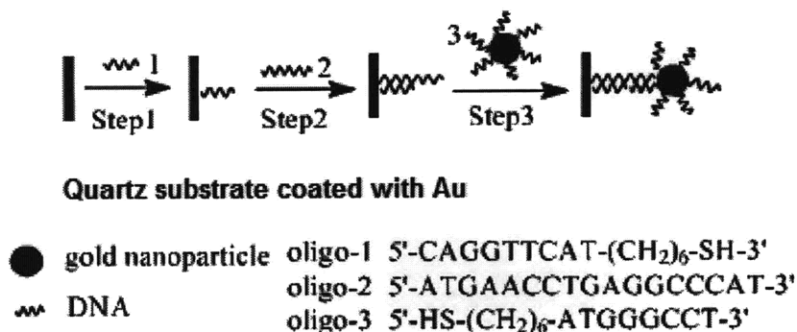


Figure 4-1 Procedure of amplified assay of a target DNA by oligonucleotide-capped gold nanoparticle using Quartz Crystal Microbalance detection [47]

4.2. Electrical Detection

Change in electrical properties has also been explored as assay of DNA. In following example shown in Figure 4-2 [48], the substrate has ready-patterned electrodes with a narrow gap in between. Gold nanoparticles are anchored to substrate similarly to the process discussed in section 4.1. The nanoparticles bridge the two electrodes. Subsequent silver precipitation will lead to measurable conductivity between two electrodes.

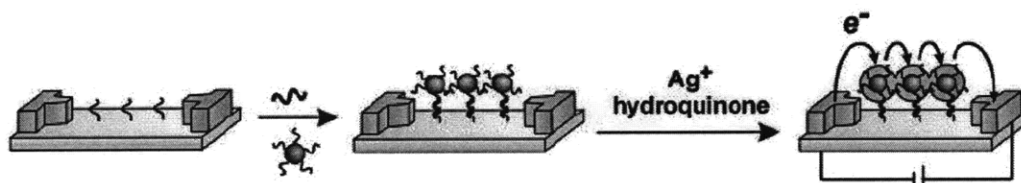


Figure 4-2 DNA assay by electrical detection [48]

4.3. Optical Detection

Because of high surface to volume ratio, metallic nanoparticles have optical properties strongly dependent on surface plasmon resonance. A optical DNA assay is developed with nanoparticles immobilized onto a glass substrate (Figure 4-3) [49]. Nanoparticles are anchored to substrate in the same way with a probe molecule and DNA. Silver precipitation is required to give visible change on the sample.

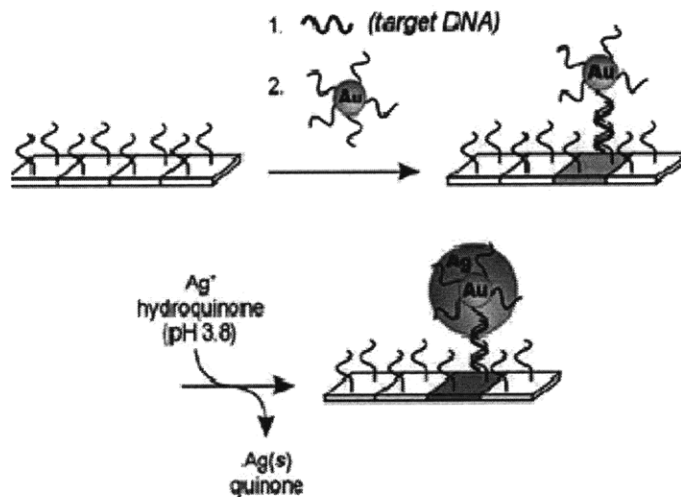


Figure 4-3 Schematic of optical detection of DNA: substrate is glass; silver ion is added to enhance the contrast [49]

In summary, current nanoparticle-based DNA detection technologies generally utilize immobilization of nanoparticles on a substrate. Common nanoparticle-based sensing mechanisms rely on quartz crystal microbalance, electrical testing and optic/visual. Compared to the other two, optical sensors are easier to use if visually observable.

5. Optical DNA Sensor Application of Stamped Nanoparticle Array

Optical behavior of metallic nanoparticles deviates remarkably from their bulk parent material. Because of high surface to volume ratio, optical properties of metal nanoparticles are determined by surface plasmon resonance. Surface plasmons are also referred as surface plasma polaritons. They are fluctuation in electron density at boundary of two materials. Plasmons are collective vibrations of an electron gas (plasma) surrounding the atomic lattice sites of a metal. Coupled with a photon, such plasmons are called polaritons. These polaritons travel along surface of metal until they decay. Excitation of surface plasmon by light is surface plasmon resonance [50].

Surface plasmon resonance is determined by shape, size, dielectric constant of material, effective mass of electron, and also dielectric constant of local environment. Attaching an analyte material on nanoparticles can change the dielectric constant of local environment surrounding nanoparticles; hence it affects the surface plasmon resonance. Metallic nanoparticles are proposed as candidate for optical sensing [51].

Whether the change in dielectric constant of local environment by attaching DNA to nanoparticle is significant to alter surface plasmon resonance that is detectable visually remains a question. This section is a technological survey on viability of using nanoparticle arrays to realize optical DNA detection.

5.1. Modeling by Electromagnetism for Single Gold Nanoparticle

Optical properties of metal nanostructure can be modeled theoretically. The breakthrough was in 1908, when Mie published a solution to Maxwell's equation that describes extinction spectra of spherical particles of arbitrary size [52]. Later experimental measurement by Kirchner and Zsigmondy is in good agreement with results from Mie's calculation.

Higher modes like quadrupole plasmon can occur for bigger nanoparticles. The nanoparticles produced by the proposed technology are expected to have small diameter and only dipole plasmon resonance is considered [53].

Dipole Plasmon Resonance Model

When a small metallic nanoparticle is in light irradiation, the electrons are under an oscillating electric field as light is electromagnetic wave in nature. The free electrons in the nanoparticle will oscillate coherently, as depicted in Figure 5-1.

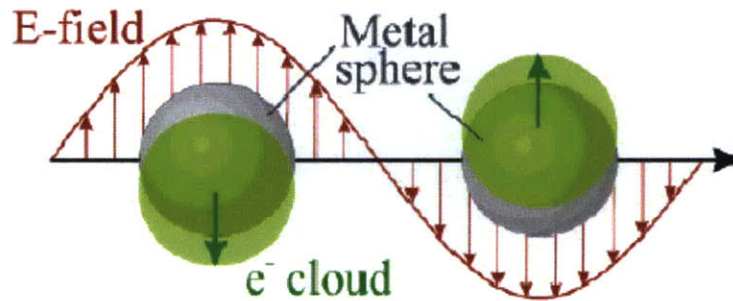


Figure 5-1 Plasmon oscillation for a sphere [53]

When the electron cloud is displaced away from the metallic nanoparticle, Coulomb attraction between electrons and nuclei acts as restoring force. Oscillation frequency depends on several factors: density of electrons, effective mass of electrons, size and shape of charge distribution, dielectric constant of particle and dielectric constant of local surrounding. Collective oscillation of electrons is called dipole plasmon resonance.

Kelly et al. examined the effect of dielectric environment on surface plasmon resonance quantitatively with simple electromagnetic theories and models [53]. For spherical particles with its size much smaller than wavelength of light it is interacting, electric field of light can be taken

to be constant in the modeling. Electrostatics, instead of electrodynamics, dominates interaction of light and plasmons, according to Quasistatic Approximation [53].

Assume incident light has electric field of E_0 , and it is in x direction, $E_0 = E_0\hat{x}$, \hat{x} is the unit vector. Electric displacement D is defined as $D = \epsilon E$. Laplace's equation

$$\nabla^2\varphi = 0$$

where φ is electric potential. Electric field E is related to electric potential φ by

$$E = -\nabla\varphi$$

Two boundary conditions are

- i. φ is continuous at nanoparticle surface
- ii. normal component of electric displacement D is continuous

The general solution to Laplace's Equation has angular solutions.

$$\varphi = A r \sin\theta \cos\phi \text{ inside the nanoparticle } (r < a)$$

$$\varphi = \left(-E_0 r + \frac{B}{r^2}\right) \sin\theta \cos\phi \text{ outside the nanoparticle } (r > a)$$

where A and B are constants that can be determined from boundary condition.

$$E_{out} = E_0\hat{x} - \alpha E_0 \left[\frac{\hat{x}}{r^3} - \frac{3x}{r^5} (x\hat{x} + y\hat{y} + z\hat{z}) \right]$$

where α is sphere polarizability, $\hat{x}, \hat{y}, \hat{z}$ are unit vector. The first term is the applied field, and the second term is induced dipole field from polarization of free electrons.

For a sphere, polarizability is

$$\alpha = g_d a^3$$

with g_d defined as

$$g_d = \frac{\epsilon_i - \epsilon_o}{\epsilon_i + 2\epsilon_o}$$

The extinction (absorption + scattering) efficiency calculated by Kelly et al. is

$$Q_{ext} = 4xIm(g_d)$$

where

$$x = \frac{2\pi a \sqrt{(\epsilon_o)}}{\lambda}$$

From theoretical modeling results by Kelly, the results show that extinction efficiency does depend on local dielectric environment ϵ_o . However, the difference in dielectric constant between air and organic material is not large. Moreover, before binding DNA, nanoparticle is already capped with a layer of monole that bonds DNA. The change of dielectric environment by bonding of DNA is limited because of pre-existing DNA “probe” molecule.

There are some limitations in the model

- It only deals with single nanoparticle; interactions between particles are not considered.
- Substrate effect is ignored.
- Nanoparticles are not perfectly spherical in practice, especially on a substrate.
- There are some simplifications are employed in the analysis.

5.2. Previous Experimental Work on Single Nanoparticle

As discussed previously, calculation shows that optical properties of nanoparticle depend on local dielectric environment. Later experiments agree with the calculation and further explore its application as biosensor [54-56].

Mock et al. studied effect of dielectric environment on surface plasmon resonance of silver nanoparticles [55]. The nanoparticles have average size around 70 nm. However, besides spherical nanoparticles, there are also non-spherical nanoparticles with hexagonal and triangular cross sections, as characterized by TEM. Monodispersity in particle size are desired in the actual application for easier characterization. Nonetheless, the results show that there is a change in color observed after immersing nanoparticles in oil. Figure 5-2 are two dark field optical micrographs with silver nanoparticles exposed in air (A) and immersed in oil ($n=1.4$).

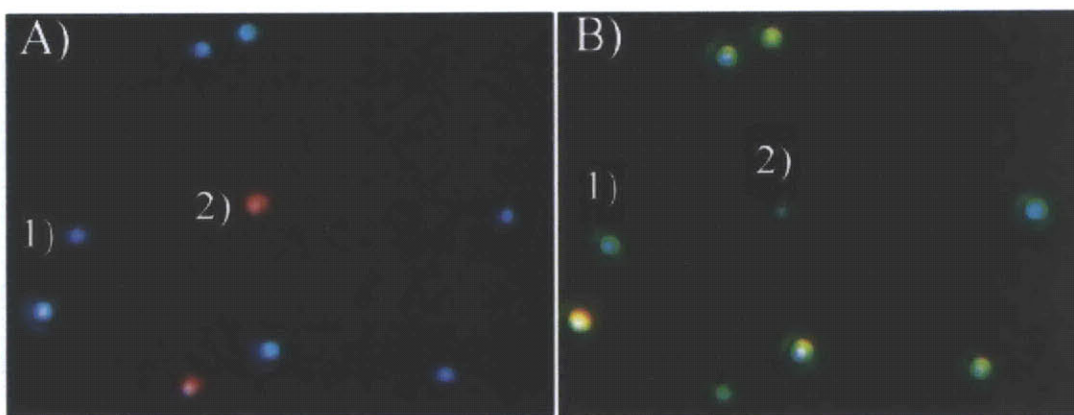


Figure 5-2 Dark field illumination with 100X objective lens (A) before immersion in oil and (B) during immersion in oil ($n=1.44$) [55]

The nanoparticles blue in color in Figure 5-2A have approximately spherical shape. The normalized scattering spectrum of particle 1 in Figure 5-2 is recorded in air (a), in oil (b) and after oil removal (c) in Figure 5-3. There is a red shift when the silver nanoparticle is exposed to a thin layer of oil, whose refractive index is around 1.4. After removal of oil, the spectrum shift back to roughly the same as the one before exposure to oil. Average peak shift for blue nanoparticles is around 52 nm.

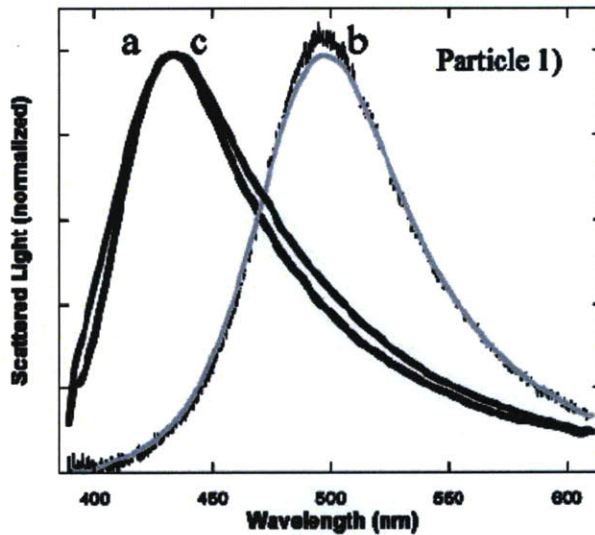


Figure 5-3 Spectra of an individual particle 1 (blue, roughly spherical) (a) before, (b) during, and (c) after exposure to thin film of 1.44 index oil [55]

A single nanoparticle biosensor was reported by Raschke et al. [54]. Figure 5-4 depicts the experiment procedure. Gold nanoparticle is functionalized with a probe-molecule that can bind analyte selectively. After adding the analyte, there is a red shift in resonance peak as shown in Figure 5-5. The solid line and the dashed line are before and after analyte bonding respectively. The shift in photon energy is 5 meV. Such small shift is indistinguishable visually; spectroscopy is required.

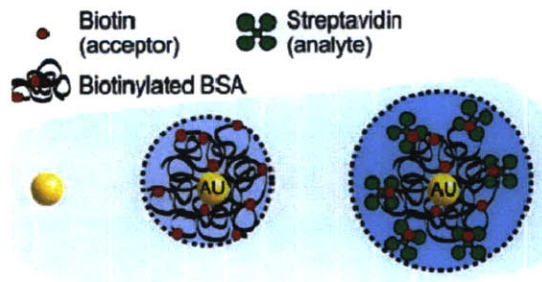


Figure 5-4 Illustration of single Au nanoparticle as streptavidin sensor [54]

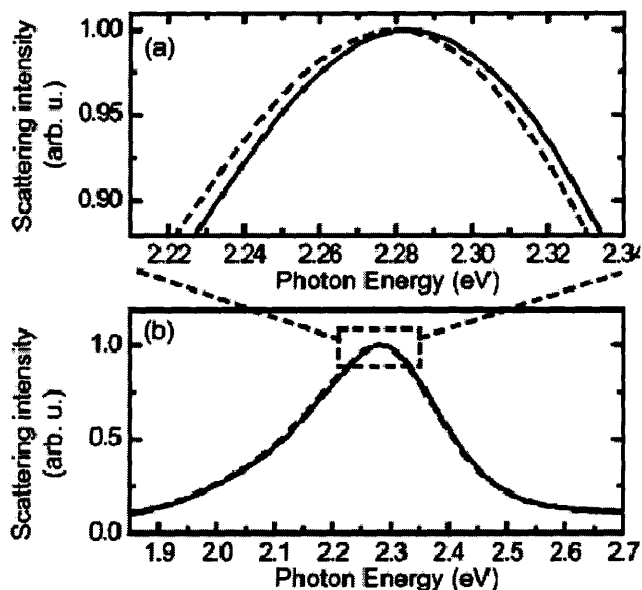


Figure 5-5 Comparison of scattering spectrum before (solid line) and after (dashed line) adding streptavidin [54]

5.3. Modeling by Fourier Modal Method (FMM) for Nanoparticle Arrays

Fourier Modal Method (FMM) [57-60] can be used for modeling optical properties of two dimensional periodic structures. With Fourier Modal Method, structure is splitted into multiple layers; permittivity within the structure is described by a Fourier expansion. It takes account interaction between structures. Complex amplitude of transmitted, reflected wave and internal field profile can be calculated [61].

Enoch et al. simulated optical properties of a gold nanoparticle 2D array using Fourier Modal Method (FMM) [62]. Figure 5-6a illustrates the structure of gold nanoparticle array used in the modeling. The particles are cylindrical with 100nm diameter and 20nm height. Figure 5-6b depicts the structure simulating change of dielectric environment by a coating with refractive index of $n=1.4$. The glass substrate has refractive index of 1.449; wavelength dependent refractive index of gold is obtained from Palik [63]. Refractive index and dielectric constant are

correlated material properties. Refractive index is used in optics, while dielectric constant is used in Maxwell's equations and electronics. They have the following relationship: $\tilde{\epsilon} = (\tilde{n})^2$, where $\tilde{\epsilon}$ and \tilde{n} are complex form of dielectric constant and refractive index.

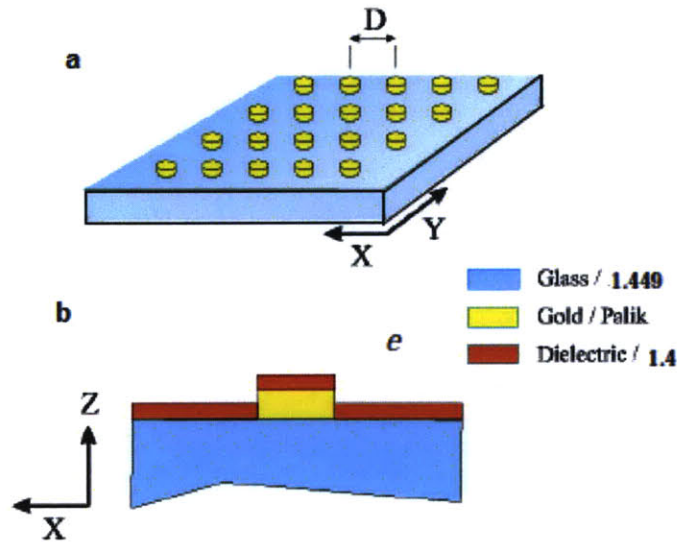


Figure 5-6 (a) Schematic description of bi-periodic gold nanoparticle array on a glass substrate, the particles are cylindrical with 100nm diameter and 20nm height; (b) Cross section of one period, covered with a layer of dielectric coating with refractive index of 1.4 [62]

With particle period D of 300nm, effect of a dielectric coating on optical extinction is simulated. The resulting extinction spectrum is shown in Figure 5-7. Local dielectric environment does have effect on surface plasmon resonance. There is a red shift in extinction peak as shown in the extinction spectrum.

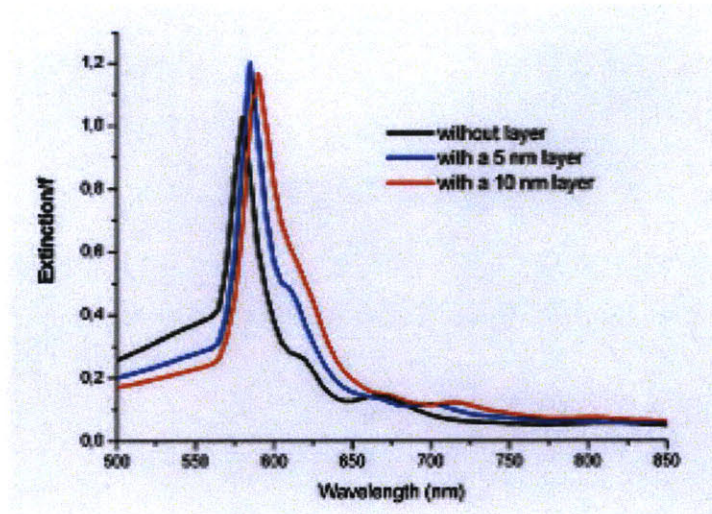


Figure 5-7 Effect of local dielectric environment calculated on optical extinction [62]

The main advantage of the Fourier Modal Method (FMM) is that it is a fast simulation technique. The limitation of this method is that it is incapable of simulating dynamic effects. And it only deals with monochromatic radiation at one time; multiple simulations are required to determine the spectrum [62].

The resonance peak shift predicted by modeling is not significantly large. Dedicated spectrometer equipments are required for characterization. This increases the final cost for end user.

5.4. Au Nanoparticle Array and Colloidal Combined DNA Sensor

Surface plasmon resonances of nanoparticles in an array are coupled by local electromagnetic interaction among the nanoparticles. The coupling effect is strongly dependent on distance between the nanoparticles. Immobilizing a nanoparticle from colloid to a nanoparticle can change the extinction spectrum significantly, as modeled by Enoch et al. [62].

A proposed DNA detection method is depicted in Figure 5-8. Firstly nanoparticle array on a solid substrate is fabricated, and nanoparticles are functionalized by a DNA probe molecule with one tip bonding to gold such as thiol group and the other end has nucleotide sequence complimentary to fragment of DNA analyte. The substrate is then exposed to solution of DNA analyte, and DNA will hybridize with the probe molecule. Finally, pre-synthesized nanoparticle colloid functionalized with a second molecule that bonds the other end of DNA analyte is added to the solution. The bonding event will immobilize the nanoparticles from colloid to nanoparticle array on the substrate. A strong surface plasmon resonance coupling is projected and shifts the resonance peak significantly to be observable visually.

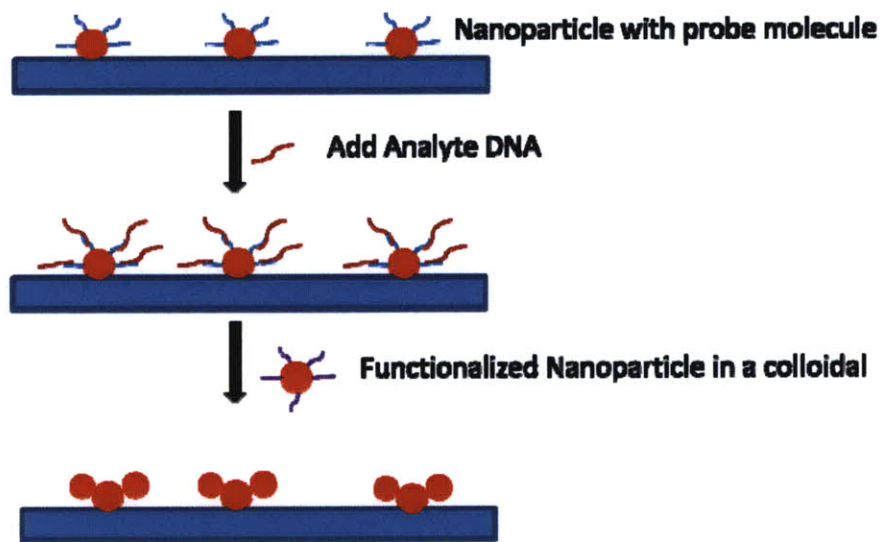


Figure 5-8 Schematic of proposed DNA sensor with combined nanoparticle array and colloid (Drawing is not to scale)

Cost of stamped nanoparticle array by method 1 is estimated as shown in appendix. The cost drops quickly as production volume increases, as depicted in Figure 5-9. At full capacity, the cost estimated is US\$ 1.8. Compared to DNA detection method described in section 4.3, the proposed method has an increase in cost by US\$ 1.8. With recycle of silicon substrate with

inverted pyramids or other proposed methods, the cost is even lower. The increase in cost is tolerable and this technology is expected to have higher sensitivity.

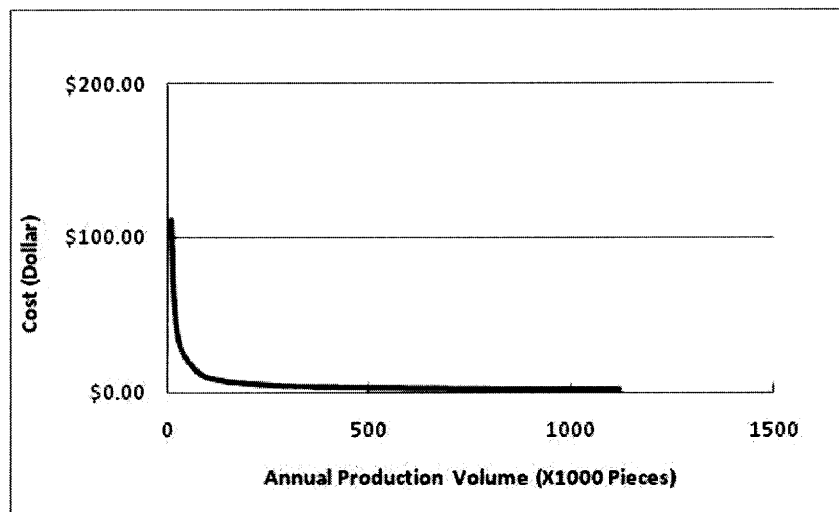


Figure 5-9 Modeled unit cost versus production volume

In summary, both modeling and experiment prove that nanoparticle can sense change of dielectric constant at immediate environment. There are biosensors being developed based on this principle. For ease of use and reliability of detection, monodispersity in size and shape is required.

Surface plasmon resonances of individual particles in the array are coupled by electromagnetic interaction. Change of local dielectric constant not only affects surface plasmon resonance of individual particles, but also affects coupling effect of local field. However, the resonance peak shift may not be very large.

Another sensor mechanism is proposed. DNA detection is viable by anchoring nanoparticles from colloid solution onto nanoparticle array. This method has higher cost compared to optical detection method introduced in section 4.3, but increase in cost is not very high.

6. Intellectual Property Assessment

Intellectual property assessment is essential while evaluating a new technology. New technologies cannot be implemented in the market directly if there are existing intellectual properties related to the technology filed by other entities. It helps to avoid potential legal issues by identifying existing intellectual properties. In addition, it is of great importance to make sure the technology can be protected by filing intellectual property like patent. Patent, the most important form of intellectual properties, offers intellectual property protection for twenty years.

This chapter aims to identify any intellectual properties which pose obstacles to the technology being evaluated. The United States Patent Office database is the primary source for the survey here.

There are many relevant patent filed on interference lithography and soft lithography. The two fundamental patents are:

- US Patent# 5512131 Formation of microstamped patterns on surfaces and derivative article, by Kumar et al, Harvard 1993 Patent on contact printing soft lithography
- US Patent# 6882477 Method and system for interference lithography utilizing phase-locked scanning beams, by Schattenburg et al, MIT 2000 Patent on interference lithography

The strategies to overcome these problems are:

- The patent on soft lithography was filed in year 1993. It is going to be expired by the time when this technology is developed.

- The patent on interference lithography was filed in 2000. However, commercial interference lithography equipment is available from equipment manufacturer; we can purchase their equipment and use it for production.

Most of the patents on transfer printing were filed in the 1970s and already expired.

- US Patent# 3632291 Transfer Printing, by Defago et al., Ciba Limited, 1969
- US Patent# 4027345, Transfer Printing, by Michio Fujisawa, et al., Toyo Boseki Kabushiki Kaisha, 1975

The specific application requires more intellectual properties on structure, design, fabrication etc.. For DNA detection using nanoparticles, there is an existing patent, US patent 6750016, filed by Mirkin et al.. They claimed nucleic acid detection by nanoparticles attached with oligonucleotides with sequences complementary to portions of the sequence of the nucleic acid.

The new feature in terms of DNA detection from this proposed technology being assessed is that it uses nanoparticle array as substrate, the interaction of nanoparticle on substrate and nanoparticle immobilized from colloid changes the optical properties like color. It is expected to have higher sensitivity as coupling strongly affects the extinction spectrum.

In summary, intellectual property survey did not found severe barrier for this nanoparticle array patterning technology. However, its application as DNA detection requires more effort on intellectual property. Negotiation and licensing with existing patent holder may be required.

7. Conclusion

Synergizing interference lithography, soft lithography and self assembly, a novel stamped nanoparticle array technology is capable of fabricating nanoparticle arrays in parallel on a large scale. It is more cost competitive compared to other approach like optical lithography, electron beam lithography or serial writing process like dip pen lithography.

Among several possible applications, potential as DNA sensor is investigated as focus in this project. Immobilizing DNA to nanoparticles will change the local dielectric environment, and shift its surface plasmon resonance peak. In this way, it can function as a DNA assay. Spectroscopy may be required as the peak shift predicted is not large. Another DNA detection method based on nanoparticle is proposed. It detects DNA by anchoring nanoparticles from colloid to nanoparticle arrays on the substrate. The coupling effect within nanoparticles will shift resonance peak significantly, and hence alter the color of the device. There is an increase in cost compared to other optical DNA assay. However, cost analysis shows that the increase in cost is tolerable.

There is no intellectual property barrier which endangers the technology as a method to fabricate nanoparticle array. Application as DNA sensor will require collaboration with existing patent.

As this technology is at its very embryonic stage, there are some limitations in the survey of this project. This paper employed theoretical modeling and relevant experiment results from previous research by other people; the device structure etc. may not be identical. The complex biochemistry and molecular dynamics behind DNA detection is not discussed here. The time frame also presents uncertainty to development of this technology.

8. References

1. *International Technology Roadmap for Semiconductors: Lithography*. 2007.
2. Ng, W.W., C.-S. Hong, and A. Yariv, *Holographic interference lithography for integrated optics*. IEEE Transactions on Electron Devices, 1978. **25**(10): p. 1193-1200.
3. Schattenburg, M. and P.N. Everett, *Method and system for interference lithography utilizing phase-locked scanning beams*. 2000, Massachusetts Institute of Technology: US.
4. Cheng, J.Y., A.M. Mayes, and C.A. Ross, *Nanostructure engineering by templated self-assembly of block copolymers*. Nat Mater, 2004. **3**(11): p. 823-828.
5. Rogers, J.A. and R.G. Nuzzo, *Recent progress in soft lithography*. Materials Today, 2005. **8**(2): p. 50-56.
6. Smith, H.I., *Submicron- and Nanometer-structures Technology*. 1994, Sudbury, MA.: NanoStructures Press.
7. Castaño, F., *Templates fabrication using Interference Lithography*. 2008, Massachusetts Institute of Technology: Cambridge, MA.
8. Rayleigh, L., Proc. London Math. Soc., 1879. **10**: p. 4.
9. Nichols, F.A. and W.W. Mullins, Trans. Metall. Soc., 1965. **233**: p. 1840.
10. Frantzeskakis, E., *Analysis of Potential Applications for the Templated Dewetting of Metal Thin Films*, in *Department of Material Sciencen and Engineering*. 2005, Massachusetts Institute of Technology: Cambridge MA.
11. Mullins, W.W., J. Appl. Phys., 1959. **30**: p. 77.
12. Jiran, E. and C. Thompson, *Capillary instabilities in thin films*. Journal of Electronic Materials, 1990. **19**(11): p. 1153-1160.
13. Giermann, A.L. and C.V. Thompson, *Solid-state dewetting for ordered arrays of crystallographically oriented metal particles*. Applied Physics Letters, 2005. **86**(12): p. 121903.
14. Choi, W.K., et al., *A Combined Top-Down and Bottom-Up Approach for Precise Placement of Metal Nanoparticles on Silicon 13*. Small, 2008. **4**(3): p. 330-333.
15. Xia, Y. and G.M. Whitesides, *Soft Lithography*. Angewandte Chemie International Edition, 1998. **37**(5): p. 550-575.
16. Love, J.C., et al., *Self-Assembled Monolayers of Thiolates on Metals as a Form of Nanotechnology*. Chemical Reviews, 2005. **105**(4): p. 1103-1170.
17. Kumar, A. and G.M. Whitesides, *Features of gold having micrometer to centimeter dimensions can be formed through a combination of stamping with an elastomeric stamp and an alkanethiol "ink" followed by chemical etching*. Applied Physics Letters, 1993. **63**(14): p. 2002-2004.
18. Xia, Y., et al., *Complex Optical Surfaces Formed by Replica Molding Against Elastomeric Masters*. Science, 1996. **273**(5273): p. 347-349.
19. Zhao, X.-M., Y. Xia, and G.M. Whitesides, *Fabrication of three-dimensional microstructures: Microtransfer molding*. Advanced Materials, 1996. **8**(10): p. 837-840.
20. Kim, E., Y. Xia, and G.M. Whitesides, *Polymer microstructures formed by moulding in capillaries*. Nature, 1995. **376**(6541): p. 581-584.
21. King, E., et al., *Solvent-assisted microcontact molding: A convenient method for fabricating three-dimensional structures on surfaces of polymers*. Advanced Materials, 1997. **9**(8): p. 651-654.

22. Cao, Y., *Design and Prototype-A Manufacturing System for the Soft Lithography Technique*, in *Department of Mechanical Engineering*. 2006, Massachusetts Institute of Technology: Cambridge.
23. Delamarche, E., et al., *Stability of molded polydimethylsiloxane microstructures*. *Advanced Materials*, 1997. **9**(9): p. 741-746.
24. Sharp, K.G., et al., *Effect of Stamp Deformation on the Quality of Microcontact Printing: Theory and Experiment*. *Langmuir*, 2004. **20**(15): p. 6430-6438.
25. Hui, C.Y., et al., *Constraints on Microcontact Printing Imposed by Stamp Deformation*. *Langmuir*, 2002. **18**(4): p. 1394-1407.
26. Schmid, H. and B. Michel, *Siloxane Polymers for High-Resolution, High-Accuracy Soft Lithography*. *Macromolecules*, 2000. **33**(8): p. 3042-3049.
27. Odom, T.W., et al., *Improved Pattern Transfer in Soft Lithography Using Composite Stamps*. *Langmuir*, 2002. **18**(13): p. 5314-5320.
28. Libiouille, L., et al., *Contact-Inking Stamps for Microcontact Printing of Alkanethiols on Gold*. *Langmuir*, 1999. **15**(2): p. 300-304.
29. Geissler, M., et al., *Microcontact-Printing Chemical Patterns with Flat Stamps*. *Journal of the American Chemical Society*, 2000. **122**(26): p. 6303-6304.
30. Guo, Q., X. Teng, and H. Yang, *Nano Lett.*, 2004. **4**: p. 1657.
31. Trimbach, D., et al., *Langmuir*, 2003. **19**: p. 10957.
32. Delamarche, E., et al., *J. Phys. Chem. B*, 1998. **102**: p. 3324.
33. Loo, Y.-L., et al., *Interfacial Chemistries for Nanoscale Transfer Printing*. *Journal of the American Chemical Society*, 2002. **124**(26): p. 7654-7655.
34. Loo, Y.-L., et al., *Additive, nanoscale patterning of metal films with a stamp and a surface chemistry mediated transfer process: Applications in plastic electronics*. *Applied Physics Letters*, 2002. **81**(3): p. 562-564.
35. Loo, Y.-L., et al. *High-resolution transfer printing on GaAs surfaces using alkane dithiol monolayers*. 2002: AVS.
36. Nakao, H., et al., *Transfer-Printing of Highly Aligned DNA Nanowires*. *Journal of the American Chemical Society*, 2003. **125**(24): p. 7162-7163.
37. Menard, E., et al., *A printable form of silicon for high performance thin film transistors on plastic substrates*. *Applied Physics Letters*, 2004. **84**(26): p. 5398-5400.
38. Menard, E., R.G. Nuzzo, and J.A. Rogers, *Bendable single crystal silicon thin film transistors formed by printing on plastic substrates*. *Applied Physics Letters*, 2005. **86**(9): p. 093507.
39. Sun, Y. and J.A. Rogers, *Fabricating Semiconductor Nano/Microwires and Transfer Printing Ordered Arrays of Them onto Plastic Substrates*. *Nano Letters*, 2004. **4**(10): p. 1953-1959.
40. Cerf, A. and C. Vieu, *Transfer printing of sub-100nm nanoparticles by soft lithography with solvent mediation*. *Colloids and Surfaces A: Physicochemical and Engineering Aspects*, 2009. **342**(1-3): p. 136-140.
41. Xue, M., et al., *Transfer Printing of Metal Nanoparticles with Controllable Dimensions, Placement, and Reproducible Surface-Enhanced Raman Scattering Effects*. *Langmuir*, 2009. **25**(8): p. 4347-4351.
42. Aizenberg, J., A.J. Black, and G.M. Whitesides, *Control of crystal nucleation by patterned self assembled monolayers*. *Nature*, 1999. **398**: p. 495.

43. De Blauwe, J., *Nanocrystal nonvolatile memory devices*. Nanotechnology, IEEE Transactions on, 2002. **1**(1): p. 72-77.
44. Daniel, M.-C. and D. Astruc, *Gold Nanoparticles: Assembly, Supramolecular Chemistry, Quantum-Size-Related Properties, and Applications toward Biology, Catalysis, and Nanotechnology*. Chemical Reviews, 2003. **104**(1): p. 293-346.
45. Caruso, F., et al., *Quartz Crystal Microbalance and Surface Plasmon Resonance Study of Surfactant Adsorption onto Gold and Chromium Oxide Surfaces*. Langmuir, 2002. **11**(5): p. 1546-1552.
46. Sauerbrey, G.Z., Phys. Rev. B, 1959. **155**: p. 206.
47. Liu, T., et al., *Particle Size Effect of the DNA Sensor Amplified with Gold Nanoparticles*. Langmuir, 2002. **18**(14): p. 5624-5626.
48. Park, S.J., T.A. Taton, and C.A. Mirkin, *Array-Based Electrical Detection of DNA with Nanoparticle Probes*. Science 2002. **295** p. 1503.
49. Taton, T.A., C.A. Mirkin, and R.L. Letsinger, *Scanometric DNA Array Detection with Nanoparticle Probes*. Science, 2000. **289**(5485): p. 1757-1760.
50. Wikipedia. *Surface Plasmons*. 2009 [cited 2009; Available from: http://en.wikipedia.org/wiki/Surface_plasmon].
51. Okamoto, T., I. Yamaguchi, and T. Kobayashi, *Local plasmon sensor with gold colloid monolayers deposited upon glass substrates*. Opt. Lett., 2000. **25**(6): p. 372-374.
52. Mie, G., Ann. Phys. , 1908. **25**: p. 377.
53. Kelly, K.L., et al., *The Optical Properties of Metal Nanoparticles: The Influence of Size, Shape, and Dielectric Environment*. The Journal of Physical Chemistry B, 2003. **107**(3): p. 668-677.
54. Raschke, G., et al., *Biomolecular Recognition Based on Single Gold Nanoparticle Light Scattering*. Nano Letters, 2003. **3**(7): p. 935-938.
55. Mock, J.J., D.R. Smith, and S. Schultz, *Local Refractive Index Dependence of Plasmon Resonance Spectra from Individual Nanoparticles*. Nano Letters, 2003. **3**(4): p. 485-491.
56. McFarland, A.D. and R.P. Van Duyne, *Single Silver Nanoparticles as Real-Time Optical Sensors with Zeptomole Sensitivity*. Nano Letters, 2003. **3**(8): p. 1057-1062.
57. Bräuer, R. and O. Bryngdahl, *Electromagnetic diffraction analysis of two-dimensional gratings*. Optics Communications, 1993. **100**(1-4): p. 1-5.
58. Li, L., *Use of Fourier series in the analysis of discontinuous periodic structures*. J. Opt. Soc. Am. A, 1996. **13**(9): p. 1870-1876.
59. Li, L., *New formulation of the Fourier modal method for crossed surface-relief gratings*. J. Opt. Soc. Am. A, 1997. **14**(10): p. 2758-2767.
60. Nevière, M. and E. Popov, *Light propagation in periodic media : differential theory and design*, ed. M. Dekker. 2003. , New York.
61. *Rigorous Domain Research* [cited 2009 July 02]; Available from: http://www.phy.hw.ac.uk/resrev/rd_research.htm.
62. Enoch, S., R. Quidant, and G. Badenes, *Optical sensing based on plasmon coupling in nanoparticle arrays*. Opt. Express, 2004. **12**(15): p. 3422-3427.
63. Lynch, D.W. and W.R. Hunter, *Handbook of optical constants of solids*, ed. E.D. Palik. 1985, New York: Academic Press.

9. Appendix

Cost Model

Cost of product is vital factor in the market. A process-based cost model is presented here for this stamped nanoparticle array patterning technology. It take accounts fixed cost and variable cost. Fixed cost consists of equipment (interference lithography, evaporator, stamping station, spin coater, annealing furnace etc), tools and plant; variable cost includes material (Silicon wafer, PDMS, gold source, photoresist, developer, etchant etc.), energy and labor. The resources required are required from each process step.

Estimated cost is plotted in following figure. The cost drops quickly as production volume increases. At full capacity, the cost estimated is US\$ 1.8.

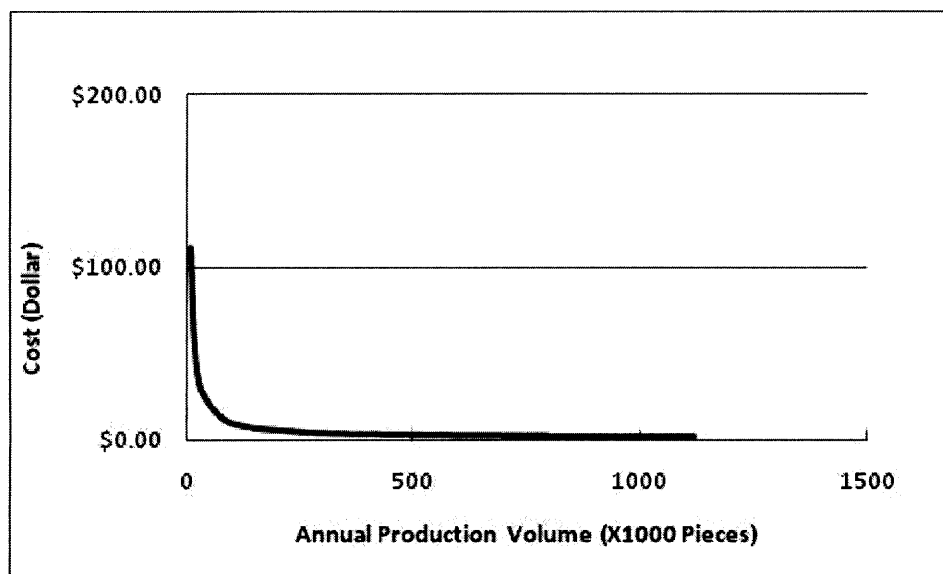


Figure 9-1 Modeled unit cost versus production volume

Some parameters used in the model are listed in following table. The plant and equipment cost are dispersed in five years. Overhead cost is estimated to be 20% of fixed cost. The annual production capacity estimated is 7200 wafers (6 inch in diameter). Each wafer can be diced to

160 pieces (1x1cm) used for final product. The final annual production capacity is 1.15 million pieces.

Table 2 Information used in cost modeling

Plant	Price	Quantity
	\$ 2,000,000	1
Equipment	Price	Quantity
IL,	\$ 20,000	1
evaporater,	\$ 400,000	1
Stamp station,	\$ 50,000	1
spin coater,	\$ 150,000	1
Oven	\$ 200,000	1
Others	\$ 50,000	1
Material	/wafer	
Si wafer 6"	\$ 30	
Photoresist/developer/SC/etchant	\$ 4	
Energy	\$ 1	
Au	\$ 120	
PDMS	\$ 10	
Labor	AverageAnnual wage	Quantity
	\$ 20,000	10